arXiv:cond-mat/0508285v1 [cond-mat.mes-hall] 11 Aug 2005

Anomalous quantum chaotic behavior in nanoelectromechanical structures

Luis G. C. Rego[1], Andre Gusso[2], and M. G. E. da Luz[2]
1-Departamento de Física, Universidade Federal de Santa Catarina, Florianópolis, SC, 88040-900, Brazil,
2-Departamento de Física, Universidade Federal do Paraná, Curitiba, PR, 81531-990, Brazil
(Dated: February 2, 2008)

It is predicted that for sufficiently strong electron-phonon coupling an anomalous quantum chaotic behavior develops in certain types of suspended electro-mechanical nanostructures, here represented by a thin cylindrical quantum dot (billiard) on a suspended rectangular dielectric plate. The deformation potential and piezoelectric interactions are considered. As a result of the electron-phonon coupling between the two systems the spectral statistics of the electro-mechanic eigenenergies exhibit an anomalous behavior. If the center of the quantum dot is located at one of the symmetry axes of the rectangular plate, the energy level distributions correspond to the Gaussian Orthogonal Ensemble (GOE), otherwise they belong to the Gaussian Unitary Ensemble (GUE), even though the system is time-reversal invariant.

PACS numbers: 85.85.+j, 05.45.Mt, 73.21.-b

The possibility of engineering devices at the nano and micro scales has openned a great avenue for testing fundamental aspects of quantum theory, otherwise difficult to probe in natural atomic size systems. In particular, mesoscopic structures have played an important role in the experimental study of quantum chaos [1], mainly through the investigation of the transport properties of quantum dots [2] and quantum well structures [3] in the presence of magnetic field. However, some hard to control characteristics of such structures can prevent the full observation of quantum chaotic behavior. For instance, the incoherent influence of the bulk on the electronic dynamics hinders the observation of the so called eigenstate scars [4] in quantum corrals [5]. Also, Random Matrix Theory (RMT) predictions to the Coulomb blockade peaks in quantum dots may fail due to coupling to the environment [6]. Alternatively, suspended nanostructures, due to their particular architecture, are ideal candidates for investigating as well as implementing coherent phenomena in semiconductor devices [7, 8]. In special, to understand in a controlled way how phonons influence electronic states and affect the system dynamics, possibly leading to a chaotic behavior. Such point is of practical relevance since it bears the question of stability of quantum computers [9, 10], whose actual implementation could be prevented by the emergence of chaos [11].

A remarkable characteristic of the quantum chaotic systems is the manifestation of universal statistical features that occur irrespective to their physical nature (e.g., the energy spectra of spinless particles). According to RMT the resulting spectra for systems with and without time-reversal invariance (TRI) are typically described by random matrices of the Gaussian Orthogonal Ensemble (GOE) and Gaussian Unitary Ensemble (GUE), respectively. This property was conjectured by Bohigas et al. [12] and has been firmly established by theoretical and experimental examination [1, 13]. However, there are exceptions to this rule, which consist of the special class of time-reversal invariant systems with point group irreducible representations that can exhibit the GUE statistics [14, 15]. The family of systems presently known to show this phenomenon is formed by billiards having threefold symmetry, which have been experimentally implemented [16, 17] in classical microwave cavities.

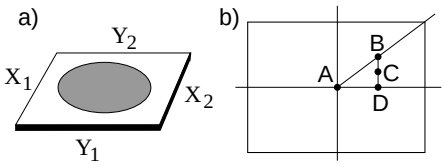

FIG. 1: a) Schematic electro-mechanical nanostruture: thin circular quantum dot on the surface of a suspended dielectric plate. b) Four different positions for the center of the quantum dot on the plate surface.

In this letter we predict that certain electro-mechanical nanostructures can also exhibit the GOE as well as the GUE spectral statistics both under TRI conditions. We consider a thin cylindrical quantum dot (billiard) suspended on a rectangular dielectric nanostructure (phonon cavity), as depicted in Fig. 1a. As the electron-phonon interaction is introduced between the electronic states, restricted to the circular quantum dot, and the phonon modes of the rectangular cavity an interesting interplay of the system's two relevant spatial symmetries takes place. In this respect, although having different dynamics, the present system resembles the much studied Sinai billiard (see, e.g., [1]), since in the later case chaos arises from the mismatch between the same two symmetries. It will be shown that for sufficiently strong electron-phonon coupling, the energy level distribution of this nanostructure exhibits the GOE spectral statistics if the center of the quantum dot lies in one of the symmetry axes of the phonon cavity, whereas the GUE statics occurs if center of the dot is located outside the symmetry axes (refer to Fig. 1b). We also investigate the influence of material and geometrical parameters on the unfolding of chaos, indicating the conditions for its experimental observation.

The boundaries of the suspended dielectric plate can be either clamped (C) or free (F), corresponding to the Dirichlet or Neumann conditions, respectively. To obtain the vibrational modes of the plate we use the Classical Plate Theory (CPT) approximation [18], which is well suited for quasi two-dimensional mechanical systems. The vibrations of the cavity are thus described by a vector field whose cartesian components are

$$U(x,y,z,t) = -z\frac{\partial W}{\partial x} \quad , \quad V(x,y,z,t) = -z\frac{\partial W}{\partial y} \ , \\ W(x,y,t) = \sum_{m,n} A_{mn} X_m(x) Y_n(y) e^{-i\omega t}. \quad (1)$$

In Eq. (1), $W(x,y,t)$ is written in terms of the one-dimensional transverse modes $X_m(x) = \sin[k_m x] + \sinh[k_m x] + \zeta_m \{\cos[k_m x] + \cosh[k_m x]\}$, and likewise for Y_n. The modes X_m and Y_n are the solutions of the Bernoulli-Euler equation [18, 19] under the appropriate boundary conditions. The kinetic and strain energies for the cavity are

$$\mathcal{K}(x,y) = \rho_{_{2D}}\, \omega^2 W^2(x,y)/2 \ , \quad (2)$$

$$\mathcal{V}(x,y) = \frac{D}{2}\left\{\left[\frac{\partial^2 W}{\partial x^2} + \frac{\partial^2 W}{\partial y^2}\right]^2 \right. \quad (3) \\ \left. - \ 2(1-\nu)\left[\frac{\partial^2 W}{\partial x^2}\frac{\partial^2 W}{\partial y^2} - \left(\frac{\partial^2 W}{\partial x \partial y}\right)^2\right]\right\} \ ,$$

where $\rho_{_{2D}}$, ν and D represent the two-dimensional density, the Poisson constant and the rigidity constant of the material, respectively. The Rayleigh-Ritz method is then used to obtain the coefficients A_{ij} of Eq. (1), by applying the condition $\partial\mathcal{U}/\partial A_{ij} = 0$ to the energy functional $\mathcal{U} = \int dxdy[\mathcal{K}(x,y) - \mathcal{V}(x,y)]$ [19]. Having obtained the vibrational eigenfrequencies (ω_α) and the eigenmodes (A^α_{mn}) of the dielectric cavity, an arbitrary deflection field is written as ($Q_\alpha(t) = Q_\alpha \exp[-i\omega t]$)

$$\mathbf{u} = \sum_\alpha \left[Q_\alpha(t) + Q^*_\alpha(t)\right]\left[U_\alpha(\mathbf{r})\,\hat{\imath} + V_\alpha(\mathbf{r})\,\hat{\jmath} + W_\alpha(\mathbf{r})\,\hat{k}\right]. \quad (4)$$

To provide the same level of description to the elastic and electronic degrees of freedom of the electro-mechanical nanostructure, we quantize the deflection field of Eq. (4). So, we define the operator $a^\dagger$ (a) that creates (annihilates) a mechanical mode as

$$a^\dagger_\alpha(t) = \sqrt{\frac{V\rho\ \omega_\alpha}{2\hbar}}\hat{Q}^\dagger_\alpha(t) - i\sqrt{\frac{1}{2\hbar V\rho\ \omega_\alpha}}\hat{P}^\dagger_\alpha(t). \quad (5)$$

Thus the quantum vibrational field that interacts with the electrons in the circular quantum dot is given by

$$\hat{\mathbf{u}} = \sum_\alpha \frac{[a_\alpha(t) + a^\dagger_\alpha(t)]}{\sqrt{2\ V\rho\ \omega_\alpha/\hbar}}\left[U_\alpha(\mathbf{r})\,\hat{\imath} + V_\alpha(\mathbf{r})\,\hat{\jmath} + W_\alpha(\mathbf{r})\,\hat{k}\right]. \quad (6)$$

The electrons, in the free electron gas approximation, occupy the states ($\kappa \equiv (\pm l, \nu)$; $l = 0, 1, 2, \ldots$)

$$\phi_\kappa(\mathbf{r}) = \frac{\mathrm{J}_l\left(\alpha_{l\nu}\frac{\rho}{R}\right)\exp[\pm il\theta]}{\sqrt{\pi}R|J_{l+1}(\alpha_{l\nu})|}\sqrt{\frac{2}{d}}\sin\left(\frac{\pi z}{d}\right). \quad (7)$$

Here, $\alpha_{l\nu}$ is the ν-th root of the Bessel function of order l, R is the radius and d the width of the quantum dot.

At low temperatures only the long wavelength acoustic modes are excited and the phonon cavity can be treated as a continuum elastic medium. Then, the relevant electron-phonon interactions are due to the deformation (DP) and piezoelectric (PZ) potentials. The DP coupling operator is written as $C_{DP}\hat{\Delta}(\mathbf{r})$, where C_{DP} is the deformation potential constant and $\hat{\Delta}(\mathbf{r}) = \nabla\hat{\mathbf{u}}(\mathbf{r})$ is the relative volume variation. The DP electron-phonon Hamiltonian is, therefore,

$$\hat{H}_{DP} = C_{DP}\sqrt{\frac{\hbar}{2V\rho}}\sum_{\kappa',\alpha,\kappa}\frac{V^{DP}_{\kappa'\alpha\kappa}}{\sqrt{\omega_\alpha}}\ b^\dagger_{\kappa'}\left[a^\dagger_\alpha + a_\alpha\right]b_\kappa \ , \quad (8)$$

$$V^{DP}_{\kappa'\alpha\kappa} = \int_{\mathcal{D}}\phi^*_{\kappa'}\nabla\left(U_\alpha, V_\alpha, W_\alpha\right)\phi_\kappa\ d\mathbf{r} \\ = -\sum_{mn} A^\alpha_{mn}\int_{\mathcal{D}} z\,\phi^*_{\kappa'}\left[X''_m Y_n + X_m Y''_n\right]\phi_\kappa\ d\mathbf{r}.$$

In Eq. (8), $b^\dagger_\kappa$ (b_κ) is the electronic creation (annihilation) operator and the integration is performed on the domain $\mathcal{D}$, defined by the boundary of the quantum dot billiard.

For a piezoelectric (PZ) nanostructure of cubic crystal symmetry, the electric field produced by the cavity vibrations is $\mathbf{E} = [(-2\varrho_{14}/\epsilon)\,\varepsilon_{xy}]\,\hat{k}$ [20], where ϱ_{14} and ε_{xy} are elements of the piezoelectric and strain tensors, respectively, and ϵ is the dielectric constant. In the CPT approximation $\varepsilon_{xz} = \varepsilon_{yz} = 0$. Thus, the piezoelectric potential is ($\Lambda = d\,(2z-d)\,/2$)

$$2\frac{\varrho_{14}}{\epsilon}\Lambda(z)\sum_\alpha\sqrt{\frac{\hbar}{2V\rho\omega_\alpha}}\left[a_\alpha + a^\dagger_\alpha\right]\frac{\partial^2 W_\alpha}{\partial x\partial y}. \quad (9)$$

The PZ electron-phonon Hamiltonian is, therefore,

$$\hat{H}_{PZ} = 2e\frac{\varrho_{14}}{\epsilon}\sqrt{\frac{\hbar}{2V\rho}}\sum_{\kappa',\alpha,\kappa}\frac{V^{PZ}_{\kappa'\alpha\kappa}}{\sqrt{\omega_\alpha}}\ b^\dagger_{\kappa'}\left[a^\dagger_\alpha + a_\alpha\right]b_\kappa \ ,$$

$$V^{PZ}_{\kappa'\alpha\kappa} = \sum_{mn} A^\alpha_{mn}\int_{\mathcal{D}}\Lambda(z)\ \phi^*_{\kappa'}X'_m Y'_n\phi_\kappa\ d\mathbf{r}. \quad (10)$$

The electro-mechanic eigenstates are thus obtained from the diagonalization of Hamiltonian $\hat{H} = \hat{H}_0 + \hat{H}_{DP} + \hat{H}_{PZ}$ written in the basis $\left\{|\phi_\kappa\rangle\prod_\alpha^N\frac{(a^\dagger_\alpha)^{n_\alpha}}{\sqrt{n_\alpha!}}\ |0\rangle\right\}$ of eigenstates of $\hat{H}_0 = \sum_\kappa E_\kappa b^\dagger_\kappa b_\kappa + \sum_\alpha^N(\hat{n}_\alpha + \frac{1}{2})\hbar\omega_\alpha$. N is the number of phonon modes included in each basis state. It can be verified that $\hat{H}$ is time reversal invariant.

We investigate the dynamical behavior of the electro-mechanical nanostructure by performing a statistical

analysis of its spectrum, in terms of: (i) the eigenenergies nearest neighbor spacing distribution $P(s)$, measured in units of mean spacing energy; and (ii) the average spectral rigidity $\overline{\Delta}_3(l)$, which provides information about the correlation between energy levels within a normalized energy interval of length l (for technical details see, e.g., Refs. [1, 13]). For all the analysis we use the first 2500 states, out of 15000 basis states, which suffice to produce very good spectral statistics.

From exhaustive calculations we found that for sufficiently strong electron-phonon coupling the observed chaotic behavior of the nanostructure proved to be quite robust with respect to variations of geometrical parameters, boundary conditions and basis size. Thus, for the sake of clearness, throughout this work we consider the representative case of a quantum dot of radius $R = 450\ nm$ and thickness $d = \delta/5$ on the surface of a square phonon cavity of sides $L = 1\ \mu m$ and width $\delta = 40\ nm$. We also assume the clamped (C) boundary conditions for the four edges of the cavity. It has been verified that the results are similar for the different boundary conditions, however the clamped only ($X_1X_2Y_1Y_2 =$\{CCCC\}) plate demonstrates more clearly the roles of the deformation potential and piezoelectric interactions. Nonetheless, the variation of some material parameters affects the chaotic behavior, for instance, the chaos is stronger for softer phonon cavities and for larger electronic effective masses. In the calculations we use the material parameters corresponding to an AlAs dielectric phonon cavity and an $Al_{0.5}Ga_{0.5}As$ quantum dot. This choice takes advantage of the very small lattice parameter mismatch of the interface as well as the large effective mass of the X valley of AlGaAs [21]. In addition, to set the necessary strength of the electron-phonon coupling we multiply the corresponding interaction potentials by an arbitrary factor β. Finally, we notice that the observed chaotic behavior does not result from the coupling a regular system (the quantum dot) with an already chaotic system (the phonon cavity). Indeed, by analyzing the spectral statistics of the vibrating plate alone we find a rather regular behavior.

The interplay between the cylindrical and rectangular symmetries, through the electron-phonon coupling, destroys the all the geometrical invariances, except for the reflection symmetries if the center of the quantum dot is located on a symmetry axis of the plate. This scenario corresponds to the points A, B and D of Fig. 1b. On the other hand, for the center of the quantum dot located at C, no symmetries remain. A slight displacement of the quantum dot is enough to generate a chaotic behavior, thus the relative coordinates used in the calculations are: A = (0,0), B = (0.05,0.05), C = (0.05,0.025), and D = (0.05,0). Figure 2 shows, for the DP interaction only and $\beta = 10$, $P(s)$ and $\overline{\Delta}_3(l)$ for these four cases. In the case A, the spectral statistics indicates a somewhat regular dynamics [22], but in B the occurrence of quantum chaos is clear and the level distributions are well described by the predictions of GOE random matrices. The same occurring for the equivalent case D. The more interesting result, however, is obtained for C, for which the statistics belongs to the GUE class, although the system is time-reversal invariant.

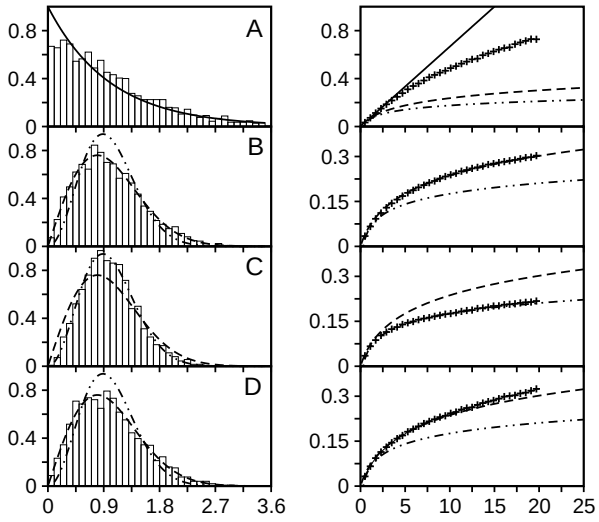

FIG. 2: The level statistics for the nanostructure with the DP interaction only and the quantum dot centered at positions A, B, C and D, Fig. 1b. The left (right) panel represents by histograms (+ symbols) the numerically calculated $P(s)$ ($\overline{\Delta}_3(l)$) distribution. The curves indicate the expected behavior for regular (solid), chaotic GOE-type (dashed), and chaotic GUE-type (dot-dashed) systems. Here $\beta = 10$.

This effect was first predicted by Leyvraz et al. [14] and observed experimentally [16, 17] in microwave billiards with only the threefold symmetry. In such case there are two classes of eigenstates: real singlets and complex conjugate doublets, which present the GOE and GUE statistics, respectively. In our case the electron states, Eq. (7), naturally provide the necessary complex representation through the angular momentum quantum number l. Note that $l = 0$ and $l = \pm1, \pm2, \ldots$ play, respectively, the role of singlet and doublet states. The coupling between electron and phonon systems is responsible for generating chaos and, according to $\hat{H}_{DP}$ and $\hat{H}_{PZ}$, the electron interacts with phonon modes α, each of definite parity. If the dot is centered at a symmetrical locus, e.g., B or D, the parity makes the Hamiltonian matrix real (up to a global phase) and the GOE statistics is obtained. When the reflection symmetry is broken, as in C, the electronic angular momenta are coupled and the Hamiltonian is complex, exhibiting the GUE statistics (a detailed analysis will appear elsewhere [23]). The same effect is obtained when the boundary conditions of the cavity are changed, which can generate, for instance, the GUE statistics in locus D for the {FFFC} nanostructure.

The dependence of the spectral rigidity $\overline{\Delta}_3(l)$ on the electron-phonon coupling strength is illustrated in Fig. 3. For the situation C and again considering only the DP interaction, we take $\beta = 1$, 3, 5, and 10. As β increases, the calculated statistics gradually converge to the GUE

prediction. Notice that the numerical results are never well fitted by the GOE case. The inclusion of more basis states does not change the observed results significantly, however, the effect is favored by changing some material parameters, for instance, by using softer phonon cavities, thiner plates, and including the PZ interaction.

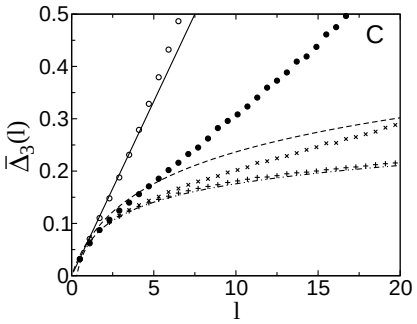

FIG. 3: The calculated spectral rigidity for case C and β equal to: 1 (open circle), 3 (filled circle), 5 ($\times$) and 10 (+). Once more the curves represent regular (solid), GOE (dashed) and GUE (dot-dashed) type of systems.

Finally, examination of equations (9) and (10) shows that, individually, both the DP and PZ interactions preserve the reflection symmetry of the matrix elements with respect to the {x,y} axes and the diagonal axes. However, when acting together the reflection invariance is broken and the spectrum statistics of loci B and D must change from GOE to GUE. Fig. 4 confirms this effect by showing the $P(s)$ distribution for the quantum dot at D, with the DP as well as PZ interactions included with $\beta = 10$. The agreement with the GUE statistics is excellent, in contrast to case D of Fig. 2. Because the AlGaAs alloy is a weak piezoelectric material, the DP coupling shows a stronger effect in promoting the chaos, whereas the main action of the PZ interaction (in the presence of DP) is to break the system's spacial symmetry.

To conclude we briefly describe results obtained for other types of suspended structures, which will be included in a forthcoming publication [23]. Regarding the

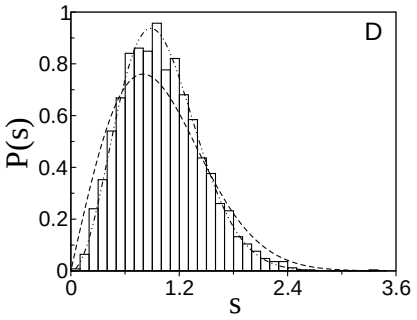

FIG. 4: The nearest neighbor spacing distribution for case D, where the DP and PZ interactions are included and $\beta = 10$ for both. The curves correspond to GOE (dashed) and GUE (dot-dashed) statistics.

phonon cavities, we investigated different boundary conditions, in particular {FFFF} and {CFCF}. The conclusions are essentially the same and the ideas presented here can be extrapolated to these distinct cases. We also considered a quantum dot of rectangular symmetry. In such case chaotic behavior was observed only for very particular asymmetric configurations, but never resulting in GUE statistics. This aspect shows the importance of the interplay between the circular symmetry of the electronic states with the rectangular symmetry of the cavity phonon modes and, therefore, the fundamental relevance of the architecture of the nanostructures.

CNPq/CT-Energ and Finepe/CT-Infra1 (M.L.), and CNPq (A.G., M.L.) are acknowledge for research grants.

[1] H. J. Stockmann, *Quantum Chaos: an Introduction* (Cambridge Univ. Press, UK, 1999).
[2] C. M. Marcus et al., Phys. Rev. Lett. **69**, 506 (1992).
[3] T. M. Fromhold et al., Phys. Rev. Lett. **75**, 1142 (1995).
[4] E. J. Heller, Phys. Rev. Lett. **53**, 1515 (1984).
[5] M. F. Crommie et al., Physica D **83**, 98 (1995).
[6] D. A. Madger et al., Physica E **6**, 382 (2000).
[7] A. N. Cleland, *Foundations of Nanomechanics* (Springer-Verlag,2002); R. H. Blick et. al., J. Phys.: Cond. Matt. 14, R905 (2002).
[8] A. D. Armour, M. P. Blencowe, and K. C. Schwab, Phys. Rev. Lett. **88**, 148301 (2002).
[9] I. L. Chuang, R. Laflamme, P. W. Shor, and W. H. Zurek, Science **270**, 1633 (1995).
[10] A. N. Cleland and M. R. Geller, Phys. Rev. Lett. **93**, 070501 (2004).
[11] B. Georgeot and D. L. Shepelyansky, Phys. Rev. E **62**, 3504 (2000); *ibid* **62**, 6366 (2000).
[12] O. Bohigas, M.J. Giannoni, and C. Schmit, Phys. Rev. Lett. **52**, 1 (1984).
[13] T. Guhr, A. M. Groeling, and H. A. Weidenmuller, Phys. Rep. **299**, 189 (1998).
[14] F. Leyvraz, C. Schmit, and H. Seligman, J. Phys. A **29**, L575 (1996).
[15] J. P. Keating and J. M. Robbins, J. Phys. A **30**, L177 (1997).
[16] C. Dembowski et al, Phys. Rev. E **62**, R4516 (2000); C. Dembpwski et al, Phys. Rev. Lett. **90**, 014102 (2003).
[17] R. Schäfer et al., Phys. Rev. E **66**, 016202 (2002).
[18] K. A. Graff, *Wave Motion in Elastic Solids* (Dover, NY, 1975).
[19] G. F. Elsbernd and A. W. Leissa, *Developments in Theoretical and Applied Mechanics*, 19-28 (1970).
[20] B. A. Auld, *Acoustic Fields and Waves in Solids* (Krieger Publishing, Florida, 1990).
[21] S. Adachi, J. Appl. Phys. **58**, R1 (1985).
[22] Calculations made for a suspended {FFFC} cavity show a well defined GOE statistics for case A.
[23] A. Gusso, M. G. E. da Luz, and L. G. C. Rego, *in preparation.*